SLAC-PUB-10291
December, 2003

Results of simulations of the PEP-II coherent instabilities. *

S. Heifets

with contributions from

K. Bane, A. Novokhatskii, G. Stupakov, R. Warnock

Stanford Linear Accelerator Center, Stanford University, Stanford, CA 94309, USA

1 Abstract

Study of conventional coherent instabilities for B-factory upgrade.

presented at PEP-II workshop, SLAC, October 2003

*Work supported by Department of Energy contract DE–AC03–76SF00515.

2 Introduction

The analytic formulas for the traditional coherent instabilities in the high-energy storage rings are summarized in [1].

The longitudinal impedance and the longitudinal wake for LER PEP-II with 8 rf cavities are illustrated in Figs. (1) and (2). The impedance is a sum of contributions of 8 rf cavities, resistive wall, and small mostly inductive components of the vacuum chamber.

The total loss factor and character of the impedance of inductive components changes substantially with the rms bunch length σ_l, see Fig. (3). The total loss is 5.4 V/pC for 11 mm and 20.08 V/pC for 6 mm.

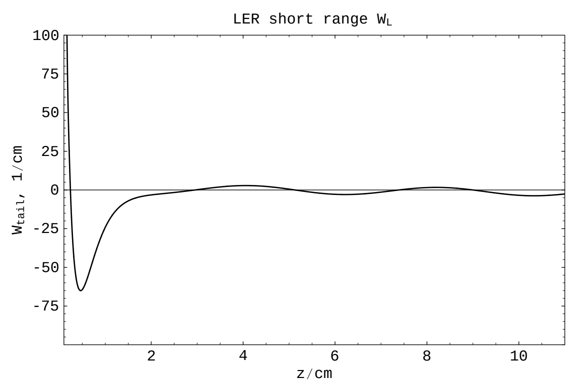

Figure 1: *LER Wake.*

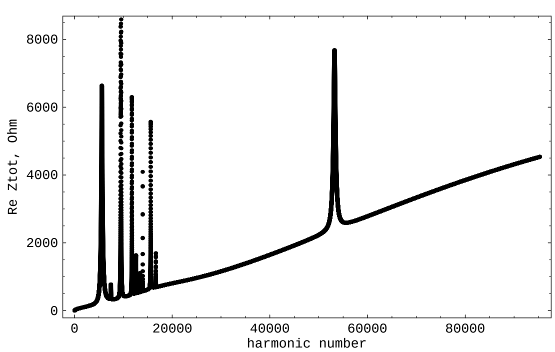

Figure 2: Real part of LER impedance vs revolution harmonics number $n = \omega/\omega_0$.

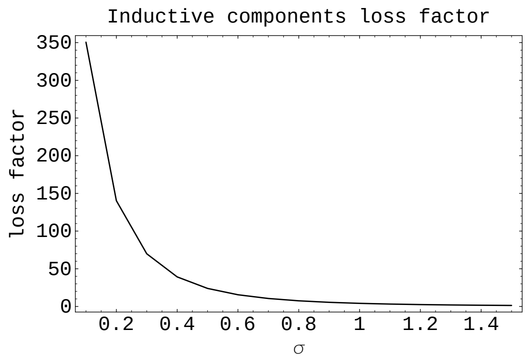

Figure 3: Loss factor V/pC of the vacuum components vs rms bunch length.

3 Longitudinal beam stability

3.1 Potential well distortion (PWD)

Haissinskii distribution is substantially different from the Gaussian distribution at nominal current. Example is shown in Fig. (4) for the zero-current rms $\sigma = 1.1$ mm and $I_{bunch} = 3.0$ mA. Curve (a) is Gaussian and curve (b) is Haissinski distributions, respectively.

Generally, the bunch lengthening is stronger at lower momentum compaction factor. This dependence is illustrated in Fig. (5) where the bunch lengthening is depicted for two values of the momentum compaction α vs bunch current. Although the lower α tends to increase the PWD as expected, the effect is small.

The PWD affects luminosity by changing the bunch shape. The effect is illustrated in Fig. (6) where the luminosity is shown in units of $L_0 = (N^+N^-c_0/4\pi s_b\sigma_x^*\sigma_y^*)$ vs hour-glass parameter $h = \sigma_l/\beta_y^*$. Three curves corresponds to (a) Gaussian bunch, and (b) Haissinski bunch at bunch currents 3 and 17 mA. In all cases the zero-current rms $\sigma_l = 11$ mm, $\alpha = 1.21E-3$. The PWD enchances the hour-glass effect.

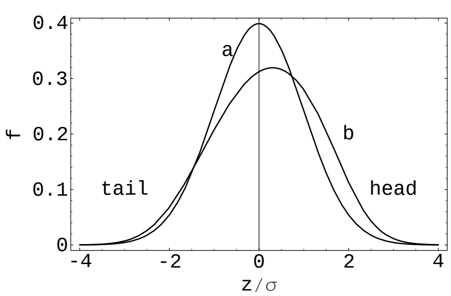

Figure 4: Potential well distortion, $I_{bunch} = 3$ mA.

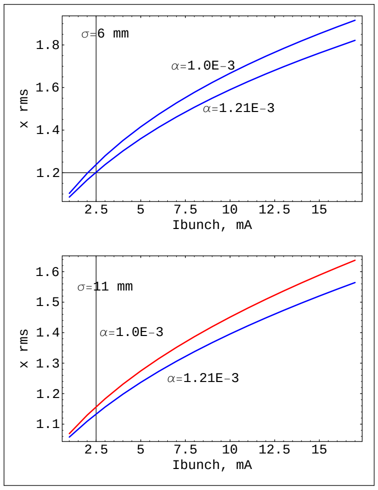

Figure 5: Dependence of the bunch lengthening on the momentum compaction α.

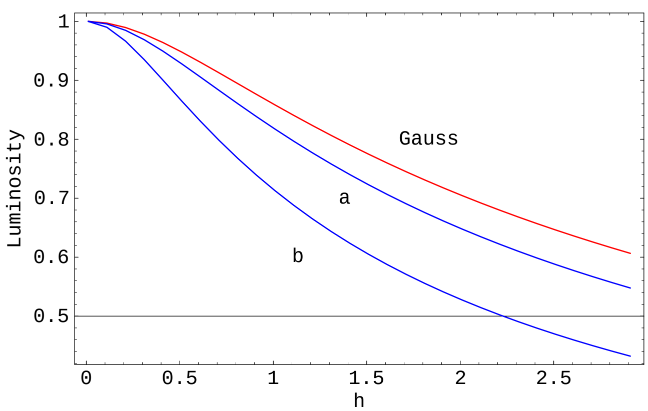

Figure 6: Luminosity $L(h)/L(0)$ vs the hour-glass parameter $h = \sigma_l/\beta_y^*$ for Gaussian bunch and for PWD distrorted bunch at the bunch current (a) 3 mA, (b) 17 mA.

3.2 Microwave instability

Additional to PWD, the rms bunch length and the energy spread increase above the threshold of the microwave instability.

The Keil-Shnell criterion estimates the threshold of the average bunch current I_{th} in terms of $(Z/n)_{eff}$. If the later is understood as $|Z(n\omega_0)|$ weighted with the first moment of the bunch spectrum $h(\omega) = x^2 e^{-x^2}$, where $x = (\omega\sigma/c_0)$, then $|Z(n\omega_0)| = 0.82$ Ohm, and $I_{th} = 2.2$ mA. Another definition of the effective impedance as absolute value of the weighted impedance, the result is almost the same, $(Z/n)_{eff} = 0.79$ Ohm. For $\sigma = 6$ mm, $(Z/n)_{eff} = 0.61$ Ohm and somewhat higher, $I_{th} = 2.9$ mA.

The tracking code was written to get more accurate estimate. The code is reasonably fast: for a given current, results can be obtained by tracking $3\,10^5$ macro particles through 70 ms (about 2 damping times) in 1 hour. The shape distortion, Fig. (3.2 agrees with that expected from Haissinskii distribution. Variation of the rms bunch length and relative energy spread (in units of the zero-current values) with bunch current is shown in Fig. (8). The energy spread starts to grow above 10 mA, much higher than the bunch current expected in the upgrades of the B-factories. It worth noting that the codes based on the direct numerical solution of the Fokker-Plank equation (A. Novokchatskii, R. Warnock) predict even higher thershold, more than 15 mA. The discrepancy partially is due to uncertainty of the definition of the threshold of instability.

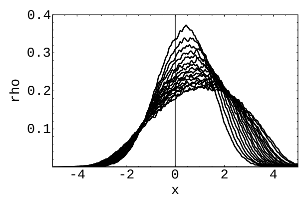

Figure 7: Particle distributions $\rho(z/\sigma_l)$ for the bunch current in the interval from 1 to 17 mA. Result of tracking with 3E5 macro particles distributed over 1000 mesh bins after 75 ms. Initial rms 11 mm.

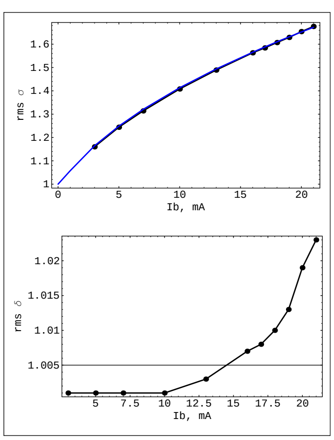

Figure 8: Variation of the energy spread and rms with current. Results of tracking with 3E5 macro particles. Initial rms bunch length is $\sigma_0 = 11$ mm. Solid line in the top figure is Haissinskii PWD.

The micro-wave instability above the threshold leads to a new equilibrium. Fig. (9) illustrates how the equilibrium is approached in time. Each curve corresponds to a bunch current in the interval from 3 to 16 mA. In this case, the code started with Gaussian distribution causing large initial oscillations. They can be reduced using pre-calculated PWD distorted initial distribution. The asymptotic rms is independent of the choice of the shape of initial distribution.

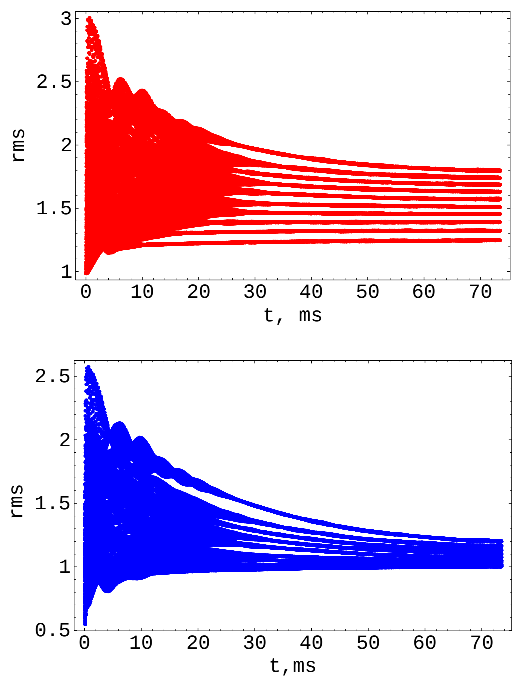

Figure 9: Variation of the rms bunch size (in red, top) and the rms energy spread (in blue, bottom) with time. Initial $\sigma = 6$ mm, $\alpha = 1.21E-3$, $\delta = 0.77E-3$. Results of tracking.

Spectra obtained by the Fourier transform of $\sigma^2(t)$, $\delta^2(t)$ and the asymmetry parameter are shown in Fig. (10) for the initial rms $\sigma = 6$ mm and $I_{bunch} = 10$ mA.

3.3 Multibunch longitudinal stability

Results describing CB dipole and quadrupole instabilities for the 1Amp beam of 1658 equidistant bunches are shown in Figs. (11) and (12) at $I_{beam} = 1$ A.

The growth rate and coherent shift are scaled proportional to the beam current. Results by MATHEMATICA, the notebook Microwave.nb. The maximum growth rate Max $(1/\tau) = (0.141/ms)\,(I_{beam}/Amp)$ for dipole modes and Max $1/\tau = 0.17\,10^{-3}\,1/ms\,(I_{beam}/Amp)$ for quadrupole modes.

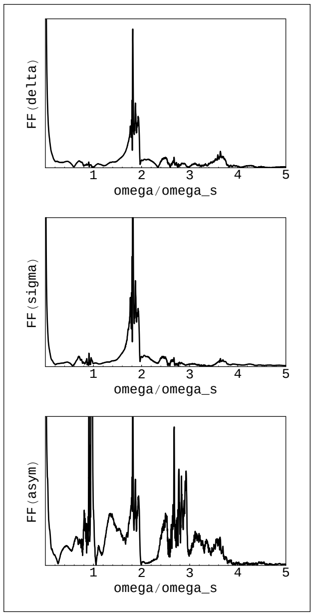

Figure 10: Spectrum of the variation of the rms σ, rms δ, and asymmetry for the initial $\sigma_0 = 6$ mm. Bunch current $I_{bunch} = 10$ mA.

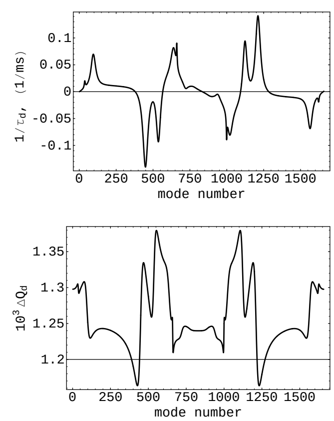

Figure 11: Dipole longitudinal CB instability, $I_{beam} = 1$ Amp

4 Transverse Instabilities

Transverse wake of asymmetric chamber changes the tune [4]. For PEP-II

$$\frac{d\nu_{x,y}}{dI_{beam}} = \pm 0.02 \, \frac{1}{Amp}. \tag{1}$$

Instability of the closed orbit (Burov et al., Burov and Stupakov) sets the threshold current

$$I_{th} = 7.2 \, Amp. \tag{2}$$

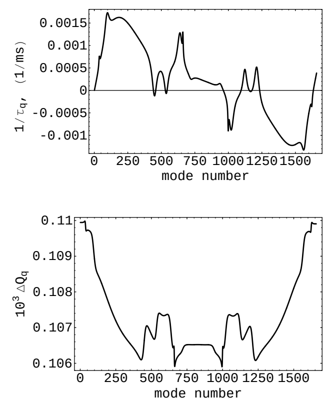

Figure 12: Quadrupole longitidinal CB instability, $I_{beam} = 1$ Amp.

Head-tail single bunch instability: the threshold of instability is about 13 mA.

Figs. (13) and (14) shows the head-tail effect for a single bunch. The feedback is off, chromaticity $\xi = 0$. Calculations are carried out using the Satoh-Chin formalism (in Fig. (13)) and CBCM formalism applied to a single bunch (in Fig. 14). Agreement of the two results is quite good.

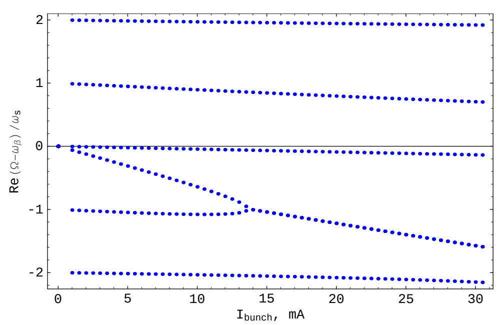

Figure 13: Head-Tail Instability, single bunch, Satoh-Chin formalism.

4.1 Transverse dipole coupled-bunch instability

The coherent tune shift and the growth rate of the fastest coupled bunch dipole modes vs beam current for 1680 equidistant bunches is shown in Fig. (15). The next figure shows growth rate and the tune shift for each CB mode.

Damping time $\tau = 30$ ms corresponds to $(\omega_0 \tau)^{-1} = 4.0\,10^{-5}$.

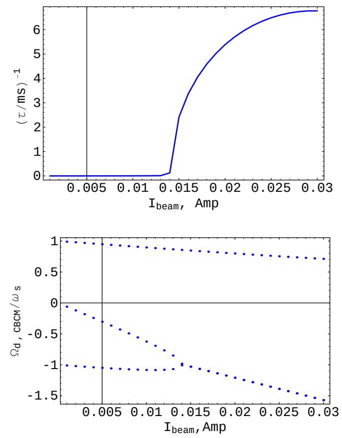

Figure 14: Head-Tail Instability, CBCM formalism applied to single bunch.

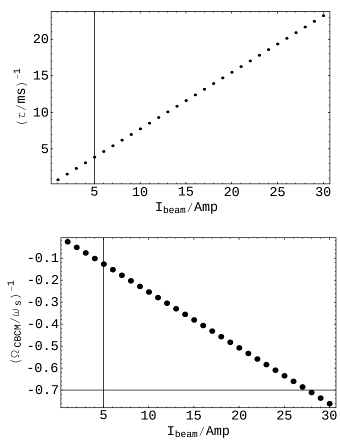

Figure 15: CB transverse dipole instability vs beam current, y-plane, $Q_y = 36.569$. $1/\tau = 0.766\, I_{beam}/Amp\ 1/ms$.

4.2 Transverse quadrupole coupled-bunch instability

4.3 Coupled-bunch Mode coupling (CBCM instability)

The CBCM theory has been developed [1] and implemented into a code. In the case of a single bunch, the results of the code agree with the Satoh-Chin theory, see Fig. (14). The coupling of dipole and quadrupole CB transverse modes can enhance the growth rate [5].

The CBCM instability is the result of crossing of modes $m = 0$ and $m = -1$ as for a single bunch. However, the crossing takes place at different currents for different CB modes as it was found by S. Berg [5] potentially reducing threshold of head-tail instability. However, for PEP-II the effect

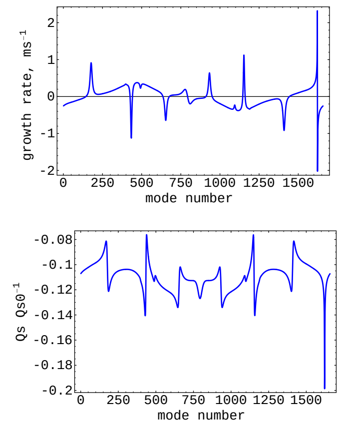

Figure 16: CB transverse dipole modes vs mode number. y-plane, $I_{beam} = 3$ A, $Q_y = 36.088$.

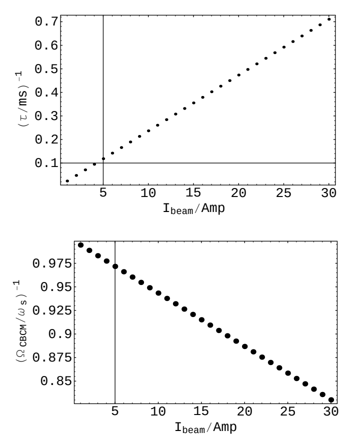

Figure 17: CB transverse quadrupole modes vs beam current. y-plane. $Q_y = 36.569$. $1/\tau = 0.023\, I_{beam}/Amp\ 1/ms$.

on the growth rate is small: for the fastest growing mode it remains almost linear with current and very close to result of the CB instability.

4.4 CBCM driven by the longitudinal instability

If the average longitudinal dipole moment is not zero due to the coupled-bunch (CB) longitudinal instability, it can affect the transverse CBCM. As an example, we consider a single unstable longitudinal CB mode with the average dipole moment d_0 and take arbitrarily the unstable mode number $\mu_0 = 2$. The beam current is 3 Amp. The FB is off. Fig. (20) shows growth rates of the dipole CB modes with $d_0 = 0$ (the red curve) and $d_0 = 3.0\,\sigma_l$ (the blue curve). The maximum growth rate is $2.32\, 1/ms$ in the first case,

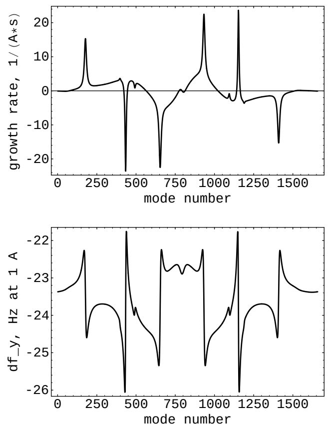

Figure 18: CB transverse quadrupole modes. y-plane. $I_{beam} = 3$ Amp. $Q_y = 36.569$.

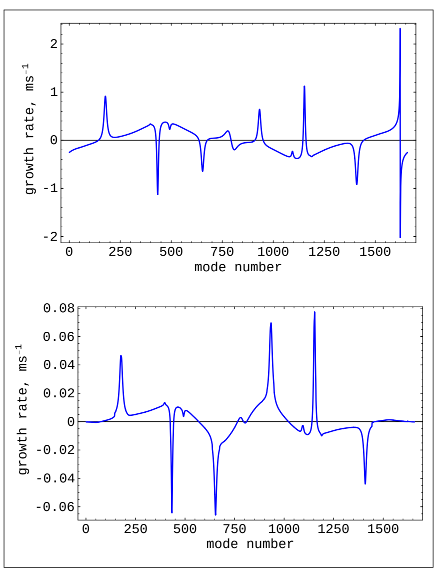

Figure 19: Growth rate of two strongest CBCM modes for 1658 bunches at 3 A beam.

and $2.54\,1/ms$ in the second case.

5 Summary

The conventional coherent instabilities are studied in the context of the plans to upgrade the PEP-II to higher luminosity mostly by increasing the total beam current with moderate increase of the bunch current and some reduction of the momentum compaction factor. Results are based on simulations with several codes written in MATHEMATICA and FORTRAN. The study

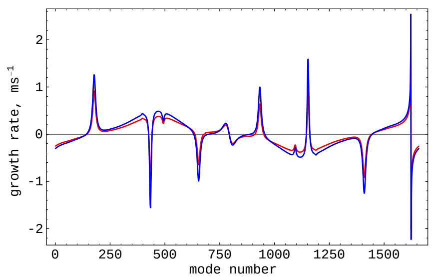

Figure 20: CBCM instability driven by the longitudinal CB instability.

shows that, in most cases, conventional instabilities will not cause problems. The single bunch thresholds are high. The CB dipole instabilities require strong feedback and, in the transverse case, to some extend are stabilized by the beam-beam tune spread. With the damping $\tau_d \simeq 50$ ms, the quadrupole mode may become dangerous above $\simeq 1$ A beam current. Although the FB detects only the dipole offset of a bunch, it produces some damping to the quadrupole modes due to the mode coupling.

References

[1] S. Heifets, A. Chao, Collection of formulas describing teh damping ring coherent instabilities. SLAC-PUB-10167, 2003

[2] A.W. Chao Physics of collective beam instabilities in high energy accelerators, J. Wiley and Sons, inc, 1993

[3] M.S. Zisman, S. Chattopadhyay, and J.J. Bisognano, ZAP user's manual, LBL-21270, UC-28, 1986

[4] A. Chao, S. Heifets, B. Zotter, Tune shifts of bunch trains due to resistive vacuum chamber without circular symmetry, Phys. Rev. ST, Volume 5, Number 11, November 2002.

[5] J. S. Berg and R.D. Ruth, Transverse instabilities for multiple nonrigid bunches in a storage ring, Phys. Rev. E, 52 (3), R2179-218, September 1995.